Progress In Electromagnetics Research M, Vol. 84, 63–72, 2019

Very-Low-Profile, Decoupled, Hybrid Two-Antenna System Using Top-Loaded, Coupled Strip Resonator for Notebook Computer Applications

Wei-Hsuan Chang and Saou-Wen Su*

Abstract—A very-low-profile, decoupled, hybrid two-antenna system top-loaded with a coupled strip resonator for isolation enhancement is demonstrated. Each hybrid antenna consists of one 2.4 GHz open slot and one 5 GHz monopole, formed on the two sides of the substrate. The two-antenna design is able to operate in the 2.4 GHz (2400–2484 MHz) and 5 GHz (5150–5825 MHz) wireless local area network (WLAN) bands and yet merely occupies a size of 5 mm × 40 mm (about $0.04\lambda \times 0.32\lambda$ at 2.4 GHz). The loaded strip resonator is employed to reduce the mutual coupling in the 2.4 GHz band. With further capacitively grounding the decoupling strip using a grounded T strip, good isolation > 18 dB over the 5 GHz bands can also be achieved. Owing to its low profile of 5 mm, the proposed design can find some practical applications in the narrow-bezel notebook computers and is of the smallest footprint among those two 2.4/5 GHz antennas for notebook applications.

1. INTRODUCTION

The popular demands for higher data rates have notably increased over a decade. This translates into the requirement of using multiple antennas inside the wireless devices to gain more spatial streams in the complex propagation environment. For instance, four wireless local area (WLAN) antennas are now deployed in the high-end gaming notebook computers to provide more antenna pattern selections for achieving better throughput performance [1]. It can be forecasted that future notebook computers will be installed with more than two WLAN antennas for the soon IEEE 11ax communications [2]. However, for antenna engineers, it becomes even more challenging to further distribute more antenna elements inside devices because very little space is left for the current notebook computers. For the rationale of limited space, conjoining two notebook antennas in close proximity (usually less than quarter-wavelength in free space [3]) becomes a feasible solution [4–8]. In this case, strong mutual coupling between the antennas needs to be sorted out first, or the degradation of sensitivity (desense) occurs in the near fields between the signal ports owing to insufficient isolation.

To improve antenna port-to-port isolation, one popular decoupling technique in common practice is to introduce additional coupling path against the original antenna coupling by inserting grounded resonator structures between the notebook antennas as in [4–8]. The decoupling structures include the uses of the meandered strip resonator [4], the T-shaped open slot in the protruded ground [5], the T-shaped decoupling structure [6, 7], and the combination of the meandered strip and the T-shaped open slot [8]. All these designs either require a minimum lateral length greater than 35 mm [7] or an antenna profile of higher than 7.5 mm [8]. These dimensions cannot fulfill the goal of accommodating more antennas in limited space and being fitted into the narrow bezels requested by recent notebook computers [9–12], in which the bezels of the notebook display can be as narrow as 5 mm.

Received 10 June 2019, Accepted 9 August 2019, Scheduled 23 August 2019
* Corresponding author: Saou-Wen Su (Saou-Wen_Su@asus.com).
The authors are with the Antenna Design Department, Advanced EM & Wireless Communication R&D Center, ASUS, Taipei 11259, Taiwan.

In this paper, we demonstrate a very-low-profile two-antenna system and yet a fully decoupled design showing the overall size of 5 mm × 40 mm (about $0.04\lambda \times 0.32\lambda$ at 2.4 GHz) only. The design consists of two identical hybrid antennas, formed by one 2.4 GHz open slot and one 5 GHz monopole antenna, printed on the bottom and the top sides of the substrate and sharing the same feed port. The open slot in this design is driven by the feed port of the monopole, and the two open slot antennas are spaced 4 mm apart. To enhance the isolation between the slots in the 2.4 GHz band, one coupled strip resonator is loaded above the monopoles for being as an additional coupling path to cancel out the original coupling [3]. For grounded resonator structures, it is to attract the surface currents on the ground plane through the grounded structures to not to enter the other antenna port. The proposed "floating" decoupling strip directly attracts the surface currents for less magnitude of currents entering the other antenna port.

The unwanted higher-order resonance of this strip resonator can interfere with the obtained operating frequencies and the isolation thereat over the 5 GHz band. By further capacitively grounding the decoupling strip near the middle (location of current null at higher-order mode) using a grounded T strip, the higher-order resonance can be removed from the 5 GHz band, and at the same time, the isolation properties over the 2.4/5 GHz bands are enhanced too. Notice that the grounded T strip is not for decoupling but for removing the higher-order resonance of the strip resonator. Nevertheless, the added T strip does help improve the isolation by about 3 dB in the 5 GHz band. Details of the design are described, and the results thereof are discussed in the article.

2. PROPOSED, HYBRID TWO-ANTENNA SYSTEM

2.1. Antenna Configuration and Design Consideration

Figure 1(a) illustrates the proposed, two-antenna system affixed to the supporting metal plate of a 14-inch notebook display, measuring 1 mm × 182 mm × 315 mm. The design is formed on a 0.4-mm-thick, flame retardant 4 (FR4) substrate ($\varepsilon_r = 4.4$) of size 5 mm × 40 mm and spaced 40 mm apart from the top-right corner of the display. This 40 mm clearance area is reserved for the mechanical structures,

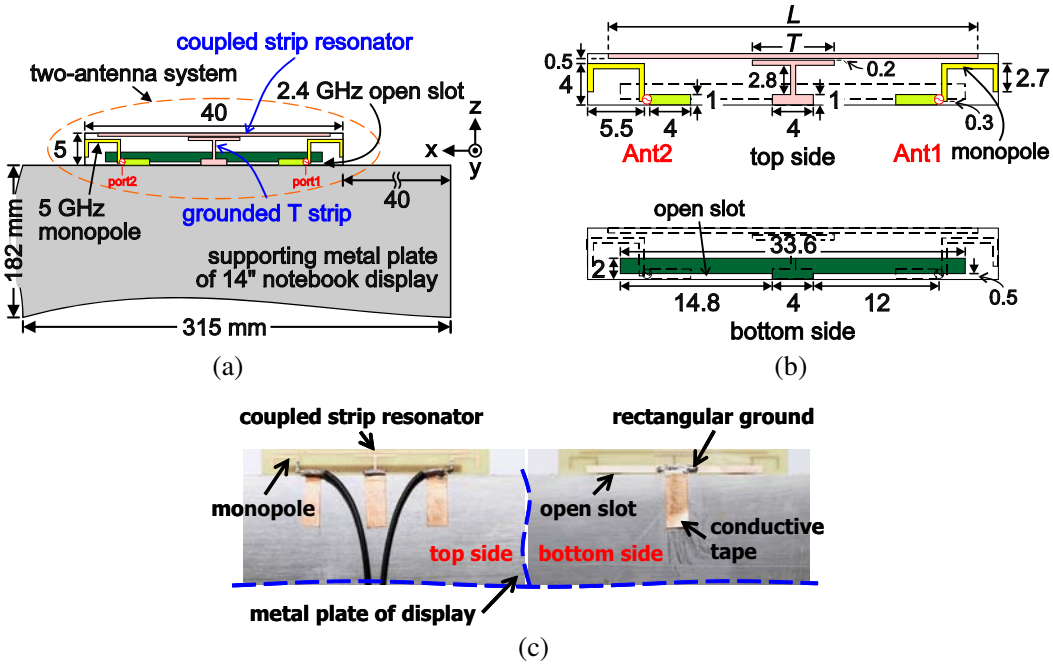

Figure 1. (a) Configuration of the hybrid, two-antenna system affixed to the supporting metal plate of a 14-inch notebook computer display. (b) Detailed dimensions of the proposed design. (c) Photos of the fabricated prototype on the top and the bottom sides.

not available for any antenna placement. The parameters of one fabricated prototype are detailed in Fig. 1(b) Each antenna (denoted as Ant1 and Ant2) is formed by one open slot and one monopole antenna, printed on the bottom and the top sides of the FR4 substrate respectively and sharing the same feed port (port1 and port2).

On the top side of the substrate are the two back-to-back inverted-L monopoles for 5 GHz operation arranged farthest apart (about 28 mm port-to-port distance here), which helps provide better isolation properties in the 5 GHz bands On the bottom side, the two back-to-back, 2.4 GHz open-slot antennas are formed in the rectangular ground of size 2 mm × 33.6 mm and spaced 4 mm apart. The open slot is capacitively driven by the feed port of the monopole, forming a hybrid of the 2.4 GHz open slot and the 5 GHz monopole antennas. The photos (top and bottom sides) of the fabricated prototype are shown in Fig. 1(c) for better understanding. Notice that the slot length in this design is 14.8 mm only, much shorter than quarter wavelength in free space (about 31 mm) required by the 2.4 GHz open slot. This is owing to the use of the coupled-fed structure for the slot antenna and the effects of the effective dielectric constant (ε_{eff} about 3.53 here for 0.4-mm FR4 substrate) [13].

Between the hybrid antennas on the top side and in the middle of the substrate are located one coupled strip resonator and one grounded T strip respectively. The strip resonator is loaded above the monopoles with a small gap of 0.5 mm and mainly helps reduce the mutual coupling between the two open slots in the 2.4 GHz band. However, this decoupling strip also contributes to the higher-order resonance around 5.7 GHz, which deteriorates the operating frequencies of the 5 GHz monopoles. By capacitively grounding the decoupling strip near the middle (location of current null at higher-order mode; see Fig. 3), the higher-order resonant mode can be shifted toward lower frequencies. The obtained 5 GHz band generated by the monopole can be retained, and the 2.4 GHz band is also unaffected. In this study, the coupled strip resonator and the grounded T strip act like a low-pass circuit for the high-band controlling for the 5 GHz monopoles.

The coupling gap between the decoupling strip and the grounded T strip is 0.2 mm, and in general, larger values of the gap can lead to higher frequencies of the higher-order resonance of the coupled

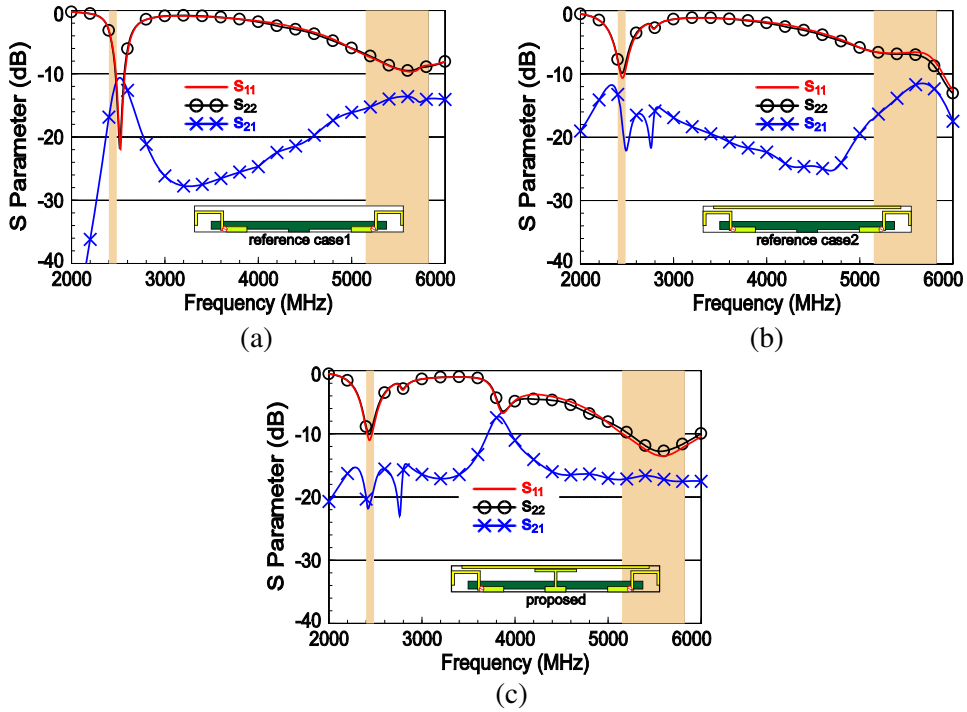

Figure 2. Simulated S-parameters (S_{11} for Ant1, S_{22} for Ant2, S_{21} isolation between two antennas) for (a) reference case 1 (proposed without any decoupling elements), (b) reference case 2 (design with coupled strip resonator only); $L = 36$ mm, and (c) the proposed design; $L = 36$ mm, $T = 8$ mm.

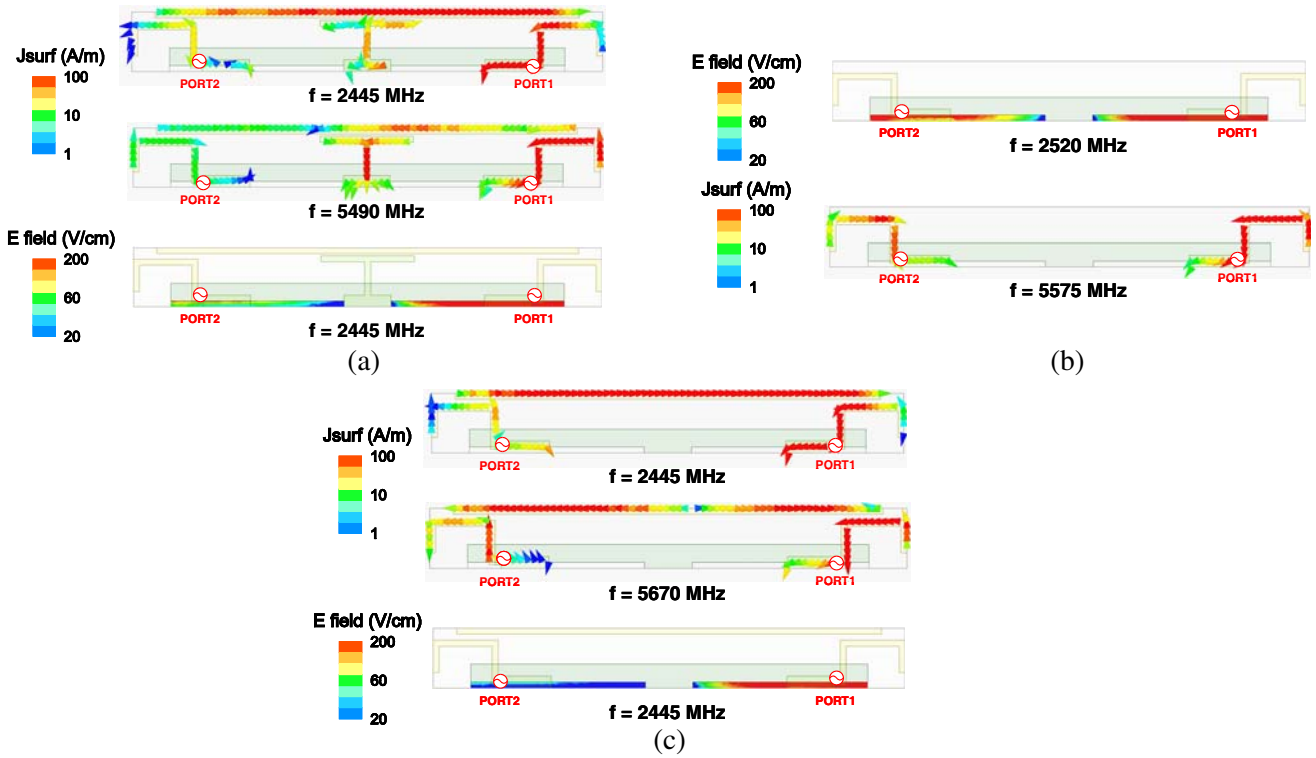

Figure 3. Simulated surface currents and electric fields for Ant1 excited at (a) 2445 and 5490 MHz in the proposed design, (b) 2520 and 5575 MHz in reference case 1, and (c) 2445 and 5670 MHz in reference case 2.

strip resonator, which is unwanted. The length L of the coupled strip resonator and the length T of the grounded T strip were also analyzed; the results will be discussed in the following section. All the widths of the strips and the slots are set constant at 0.5 mm in this design, and the nearoptimum parameters are simulated by the electromagnetic solver, ANSYS HFSS [14]. Notice that the bottom portion (size 1 mm $\times$ 4 mm) of the grounded T strip is also connected to the rectangular ground between the two slots on the bottom side via the conductive (copper) tape for the fabricated prototypes in the experiments.

2.2. Controlling Mechanisms

To better understand the decoupling mechanisms of the proposed design, the two reference cases are selected for further discussions. Figs. 2(a), (b), and (c) shows the simulated S-parameters for reference case 1 (proposed without any decoupling elements), reference case 2 (design with coupled strip resonator only), and the proposed design. The dimensions among these antennas are kept the same as those shown in Fig. 1. First for reference case 1, poor isolation (S_{21}) at about 10 dB in the lower band is obtained, and the isolation for 5 GHz operation is merely better than 13 dB. With the incorporation of the loaded strip resonator in reference case 2, the isolation enhancement (S_{21} about -13 dB, 5% less energy coupled compared with reference case 1) in the 2.4 GHz band can be achieved, but the isolation over the 5 band are degraded [see Fig. 2(b)]. This is because the additional resonance around 5.7 GHz (see S_{11}, S_{22} curves) is generated by the coupled strip resonator, which not only pushes the frequencies of the 5 GHz monopoles toward higher frequencies but also deteriorates the isolation thereat.

To remove this unwanted resonant mode from the 5 GHz band, the coupled strip resonator is capacitively grounded by the grounded T strip [see inset in Fig. 2(c)]. It can be seen in Fig. 2(c) that the higher-order resonance of the decoupling strip is now shifted to 3.8 GHz, and at the same time, the isolation properties over the 2.4/5 GHz bands can also be enhanced (about $>$ 19 and 17 dB over the 2.4 and 5 GHz bands). Notice that if the strip resonator is directly grounded (top portion of T strip merged

into decoupling strip), the isolation level in the 5 GHz band stays about the same, but for the 2.4 GHz band, the isolation becomes worse (about 5 dB). Related results are not shown here for brevity.

Figure 3(a) shows the simulated surface-current distributions and electric fields for Ant1 (port1) excited at 2445 and 5490 MHz; the arrows represent the current vectors. First at 2445 MHz, the surface currents are seen mostly populated on the couple strip resonator and the 5 GHz monopole of Ant1. Relatively strong electric fields are also found in the open slot of Ant1. These indicate that the top-loaded strip resonator effectively decouples the two 2.4 GHz open slots in the hybrid-antenna system. For port1 excitation at 5490 MHz, larger currents are distributed on the monopole, the half-portion of the strip resonator, and the grounded T strip, compared with those on the monopole of Ant2. By contrast, reference case 1 studied in Fig. 3(b) shows comparable magnitude of the electric fields in the slots and the surface currents on the monopoles between Ant1 and Ant2 at 2520 and 5575 MHz [most matched frequency points in Fig. 2(a)]. In addition, for reference case 2 in Fig. 3(c), both the surface currents and the electric fields at 2445 MHz are similar to those of the proposed design (good isolation) but the magnitude of the currents on the monopoles at 5670 MHz [largest S_{21} in Fig. 2(b)] are similar to that for reference 2. These show again that the coupled strip resonator can decouple the two 2.4 GHz open slots while it also contributes to the unwanted resonant mode in the 5 GHz band. These results from Figs. 2 and 3 suggest that with the use of the strip resonator capacitively grounded by the T strip, the isolation enhancement over the 2.4/5 GHz band for the proposed hybrid-antenna system can be achieved.

Figure 4 shows the simulated S-parameters for the proposed design as a function of the length L of the coupled strip resonator. As expected, the isolation properties in the 5 GHz band in Fig. 4(c) are not much affected, but the drop (smallest value of S_{21}) in the lower band moves toward higher frequencies as L becomes larger. This in turn influence the antenna frequencies of S_{11}, S_{22} in the 2.4 GHz band in Figs. 4(a) and (b) because the intensity of the coupling between Ant1 and Ant2 changes. Also, it is quite straightforward to see that the higher-order resonance around 3.8 GHz is affected by the length L of the strip resonator. The behavior of the S parameters with various lengths T of the grounded T strip is presented in Figs. 5(a), (b), and (c). As discussed in the paragraphs, the unwanted higher-order resonance caused by the strip resonator in the 5 GHz band can be moved toward lower frequencies. The

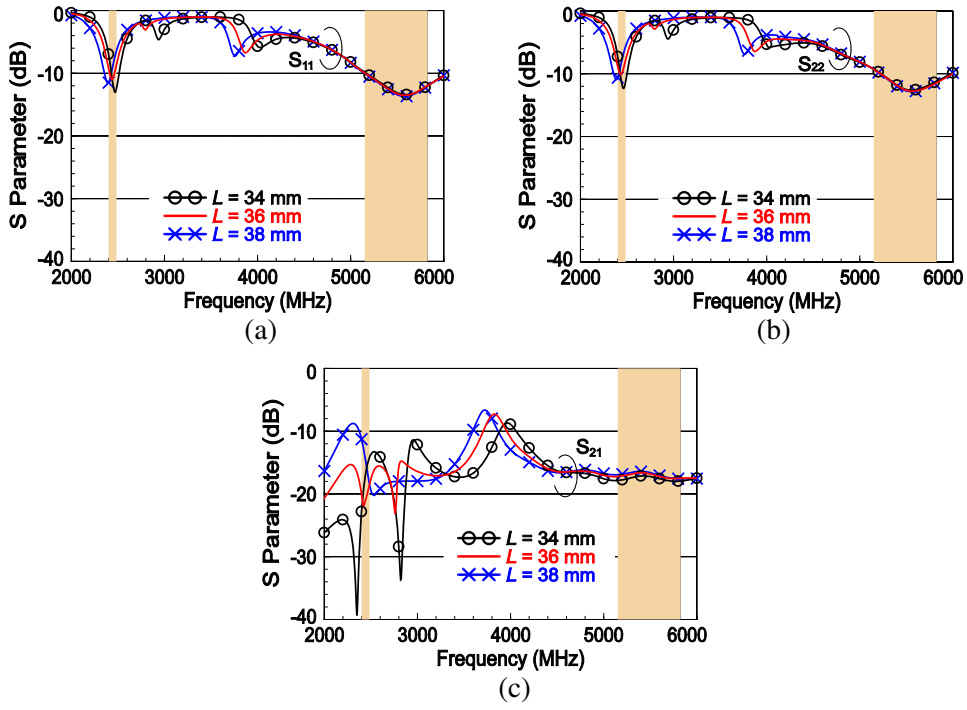

Figure 4. Simulate S-parameter for the proposed design as a function of the length L of the coupled strip resonator: (a) S_{11} for Ant1, (b) S_{22} for Ant2, and (c) S_{21} between Ant1 and Ant2.

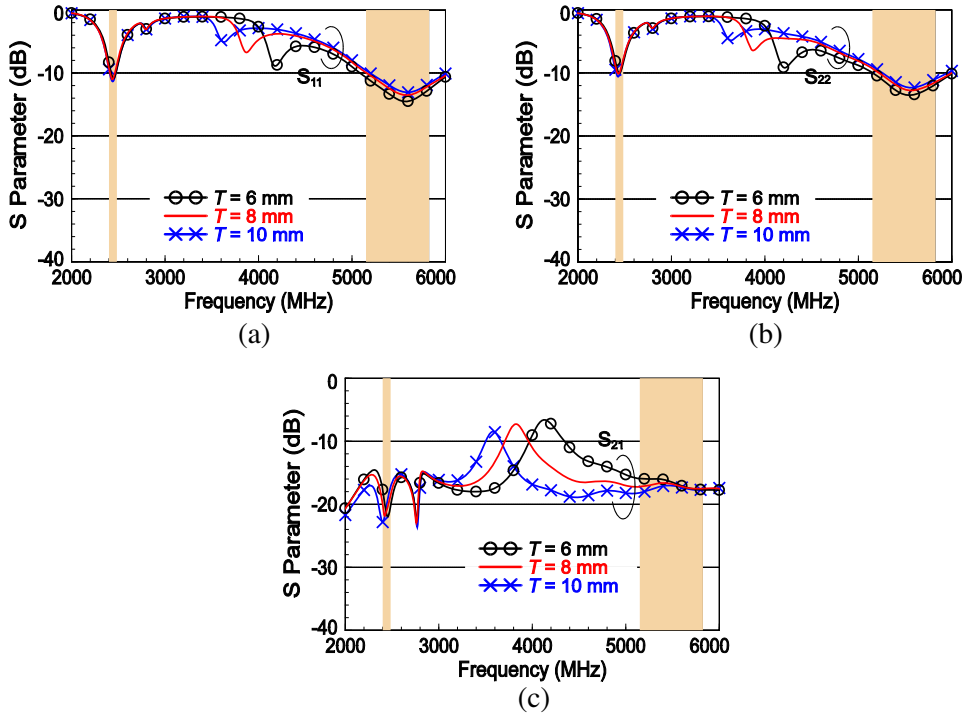

Figure 5. Simulated S-parameter for the proposed design as a function of the length T of the grounded T strip: (a) S_{11} for Ant1, (b) S_{22} for Ant2, and (c) S_{21} between Ant1 and Ant2.

larger the length T is, the poorer the S_{11}, S_{22} and S_{21} become. Also, the obtained 2.4 GHz bands of the open slots are almost unchanged, which confirms that the coupled strip resonator and the grounded T strip act like a low-pass circuit for the high-band controlling. If the length T gets further smaller (or frequencies of higher-order resonance larger than 4.2 GHz), the isolation properties over the 5 GHz band can become worse because the isolation hump (largest value of S_{21}) moves closer to the operating frequencies thereat [see tendency of S_{21} in Fig. 5(c)].

3. EXPERIMENTAL AND SIMULATION RESULTS

Figures 6(a) and (b) show the measured and simulated S-parameters for the proposed two-antenna system. The 2.4 and 5 GHz WLAN bands are marked by the shaded frequency ranges. Two 50-Ω ini-coaxial cables of length about 80 mm were used for feeding the hybrid antennas across a tiny feed gap of 0.5 mm. The inner conductor of the cable is connected to the feed point of the monopole, and the outer braided grounding is soldered to the antenna ground (size 1 mm × 4 mm) opposite to over the feed gap. It is first seen that the experimental data in general agree with the simulation. The discrepancies are due to manufacture tolerance and effects of the coaxial cables used in the experiments. The reflection coefficients of S_{11} and S_{22} in the bands of interest are all below −9.5 dB (VSWR of 2), which corresponds to about 0.5 dB transmission loss via the antenna element and is accepted for industrial WLAN notebook applications. The measured isolation (S_{21}) between the antennas is better than 17 and 18 dB over the 2.4 and 5 GHz bands, respectively.

The over-the-air (OTA) performance of the fabricated prototype was measured at our 4 m × 4 m × 4 m, SATIMO chamber of model SG 64, which uses the conical-cut method [15]. Figs. 7(a), (b) and 8(a), (b) show the measured radiation patterns in E_θ and E_φ fields for Ant1 and Ant2, respectively, at 2442 and 5490 MHz, the center frequencies of the 2.4 and 5 GHz WLAN bands. During the measurement for Ant1 or Ant2, the counterpart, Ant2 or Ant1, was terminated at the 50-Ω load. The two-dimensional (2D) radiation patterns are normalized with respect to the maximum radiation intensity in each cut. First, comparable E_θ and E_ϕ fields are seen in the x-y planes, which is advantageous for

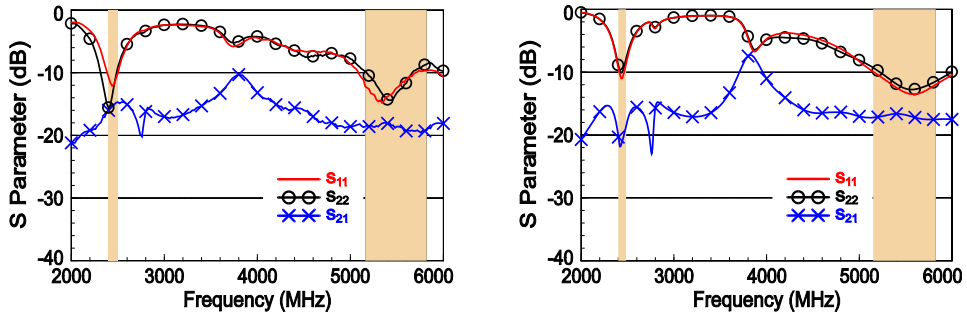

Figure 6. S parameters (S_{11} for Ant1, S_{22} for Ant2, S_{21} isolation between antennas) for the proposed, hybrid two-antenna system; $L = 36$ mm, $T = 8$ mm: (a) measured and (b) simulated results.

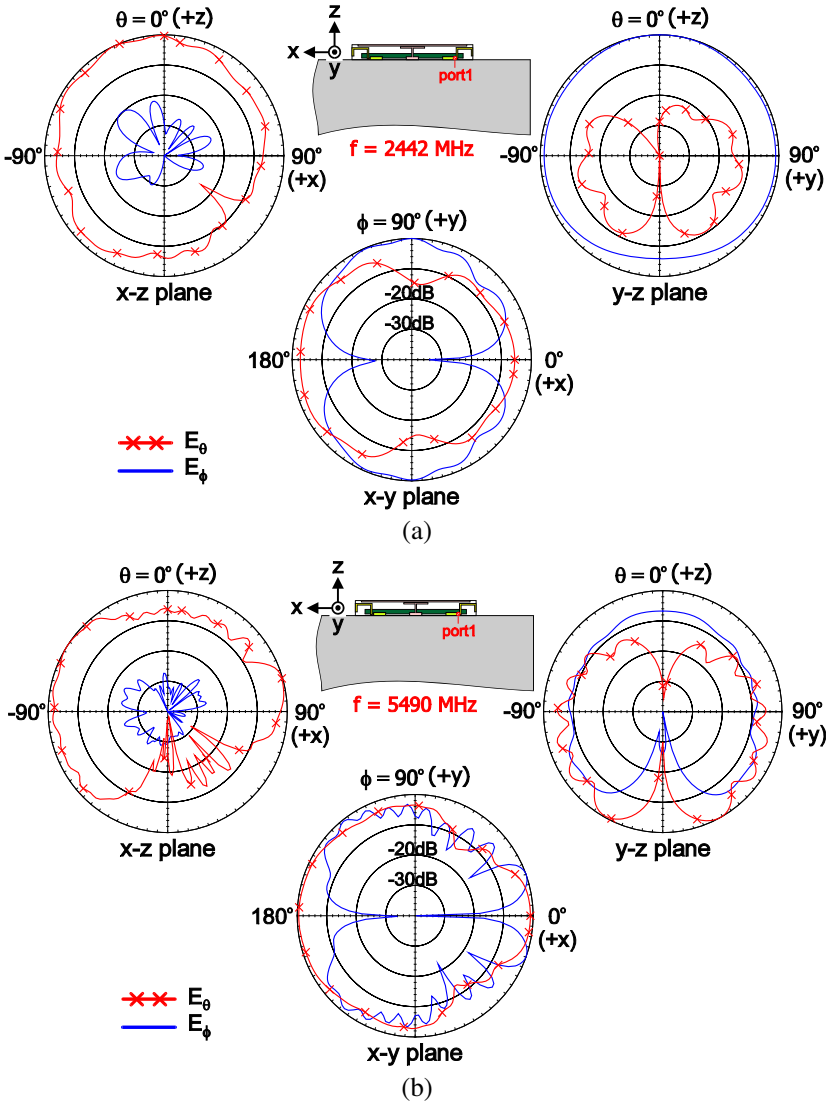

Figure 7. Measured 2D radiation patterns of Ant1 in the proposed design at (a) 2442 MHz and (b) 5490 MHz.

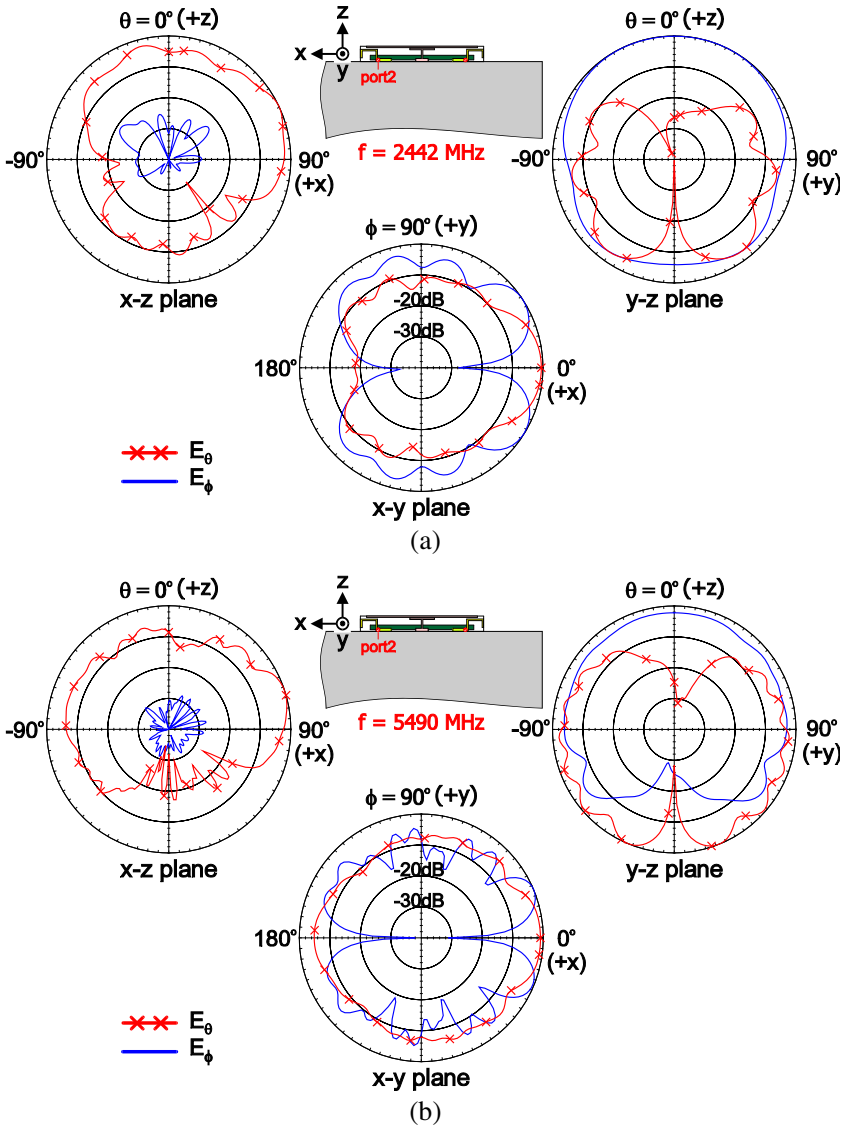

Figure 8. Measured 2D radiation patterns of Ant2 in the proposed design at (a) 2442 MHz and (b) 5490 MHz.

WLAN operation in the complex propagation environment. Second, the radiation patterns in the elevation planes (x-z and y-z cuts) in the lower band resemble those of the half-wavelength vertical patch [16]. This is probably because in addition to the open-slot radiation, the loaded strip resonator, which shows the surface currents of half-wavelength properties in Fig. 3(a), also contributes to the patch-like patterns for 2.4 GHz operation. The 5 GHz patterns are with larger radiation in the upper half-space toward the $+z$ direction above the display, similar to the radiation characteristic of the WLAN, monopole notebook antenna reported in [10].

Figure 9 plots the measured, peak antenna gain and antenna efficiency against frequency. For Ant1 in the 2.4 and 5 GHz bands, the peak gain is about 2.3 and 3.8–4.7 dBi with antenna efficiency exceeding 43% and 64%, respectively. As for Ant2, the gain is about 2.9 and 4.2–5.1 dBi with efficiency exceeding 44% and 63% in the lower and upper bands. Compared with reference 1 (proposed without any decoupling elements) shown in Fig. 2, the antenna efficiencies observed at the most matched frequency points in Fig. 2 are decreased by 0.5 dB in the lower band for reference 1 due to higher port-to-port isolation but similar to the proposed design for upper-band operation. The OTA measurement here took account of the antenna mismatch and the cable loss; the realized gain [17] and the antenna efficiency [18]

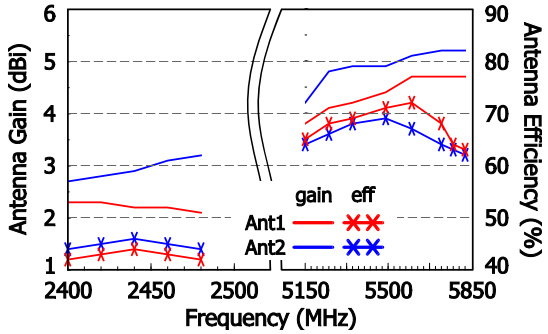

Figure 9. Measured peak antenna gain and antenna efficiency for Ant1 and Ant2 studied in Figs. 7 and 8.

are thus measured in the chamber. The antenna efficiency was also obtained by calculating the total radiated power of the antenna over the 3D spherical radiation and dividing that total amount by the input power of 0 dBm given to the antenna.

4. CONCLUSION

A novel, decoupled, hybrid two-antenna system suitable for narrow-bezel, notebook computer applications for dual-band WLAN operation has been proposed. The design comprises two hybrid antennas, one decoupling strip resonator, and one grounded T strip, all printed on a two-sided RF4 substrate of size 5 mm × 40 mm, the smallest footprint among those two-2.4/5 GHz-notebook antennas in the open literature. Each hybrid antenna has one 2.4 GHz open slot and one 5 GHz monopole antenna, sharing the same antenna feed port. The decoupling strip loaded above the monopoles helps reduce the mutual coupling in the 2.4 GHz band. With further capacitively grounding the decoupling strip using the grounded T strip, the unwanted higher-order resonance caused by the loaded strip resonator can be removed from the 5 GHz band, and at the same time, the isolation properties over the 2.4/5 GHz bands can also be enhanced. The measured port isolation is better than 17 and 18 dB over the 2.4 and 5 GHz bands. The antenna efficiency in the 2.4 and 5 GHz bands exceeds 43% and 64% for Ant1 and 44% and 63% for Ant2. Owing to the attractive features of 5-mm low profile and compactness, the proposed hybrid-antenna system is a good candidate for future multiple notebook antennas in the Gbps communications.

REFERENCES

1. RangBoost technology, ASUS, https://www.asus.com/Laptops/ ROG-Strix-Hero-II/.
2. Khorov, E., A. Kiryanov, A. Lyakhov, G. Bianchi, "A tutorial on IEEE 802.11ax high efficiency WLANs," *IEEE Comm Surveys & Tutorials*, Vol. 21, 197–216, 2019.
3. Mak, A. C. K., C. R. Rowell, and R. D. Murch, "Isolation enhancement between two closely packed antennas," *IEEE Trans. Antennas Propagat.*, Vol. 56, 3411–3419, 2008.
4. Kang, T. W. and K. L. Wong, "Isolation improvement of 2.4/5.2/5.8 GHz WLAN internal laptop computer antennas using dual-band strip resonator as a wavetrap," *Microwave Opt. Technol. Lett.*, Vol. 52, 58–64, 2010.
5. Guo, L., Y. Wang, Z. Du, Y. Gao, and D. Shi, "A compact uniplanar printed dual-antenna operating at the 2.4/5.2/5.8 GHz WLAN bands for laptop computers," *IEEE Antennas Wireless Propagat. Lett.*, Vol. 13, 229–232, 2014.
6. Liu, Y., Y. Wang, and Z. Du, "A broadband dual-antenna system operating at the WLAN/WiMax bands for laptop computers," *IEEE Antennas Wireless Propagat. Lett.*, Vol. 14, 1060–1063, 2015.

7. Chen, W. S., J. H. Shu, and C. Y. D. Sim, "Small-size WLAN/5G MIMO antenna for laptop computer applications," *Asia-Pacific Conference on Antennas and Propagat.*, 1–3, Xi'an, China, 2017.
8. Deng, J. Y., J. Y. Li, L. Zhao, and L. X. Guo, "A dual-band inverted-F MIMO antenna with enhanced isolation for WLAN applications," *IEEE Antennas Wireless Propagat. Lett.*, Vol. 16, 2270–2273, 2017.
9. Su, S. W., C. T. Lee, and S. C. Chen, "Very-low-profile, triband, two-antenna system for WLAN notebook computers," *IEEE Antennas Wireless Propagat. Lett.*, Vol. 17, 1626–1629, 2018.
10. Su, S. W., "Very-low-profile, 2.4/5-GHz WLAN monopole antenna for large screen-to-body-ratio notebook computers," *Microwave Opt. Technol. Lett.*, Vol. 60, 1313–1318, 2018.
11. Su, S. W., C. T. Lee, and S. C. Chen, "Compact, printed, tri-band loop antenna with capacitively-driven feed and end-loaded inductor for notebook computers," *IEEE Access*, Vol. 6, 6692–6699, 2018.
12. Su, S. W., "Capacitor-inductor-loaded, small-sized loop antenna for WLAN notebook computers," *Progress In Electromagnetics Research M*, 179–188, 2018.
13. Pozar, D. M., *Microwave Engineering*, 3rd Edition, Chapter 3, 143–145, Wiley, New York, 2005.
14. ANSYS HFSS, ANSYS Inc., https://www.ansys.com/Products/Electronics/ANSYS-HFSS.
15. SG 64, SATIMO, http://www.mvg-world.com/en/products/field_product_family/antenna-measurement-2/sg-64.
16. Chang, F. S., K. C. Chao, C. H. Ku, and S. W. Su, "Compact vertical patch antenna for dual-band WLAN operation," *Electronics Lett.*, Vol. 44, 612–613, 2008.
17. Volakis, J. L., *Antenna Engineering Handbook*, 4th Edition, Chapter 6, 16–19, McGraw-Hill, New York, 2007.
18. Balanis, C. A., *Antenna Theory: Analysis and Design*, 3rd Edition, Chapter 2, Wiley, Hoboken, NJ, 2012.